

Full Length Research Paper

Drying and radial shrinkage characteristics and changes in color and shape of carrot tissues (*Daucus carota L*) during air drying

Hilaire Nahimana¹, Arun S. Mujumdar² and Min Zhang^{1*}

¹State Key Laboratory of Food Science and Technology, Jiangnan University, 214122Wuxi, Jiangsu, China.

²Department of Mechanical Engineering, National University of Singapore, 9 Engineering Drive 1, Singapore 117576.

Accepted 12 August, 2011

Drying and radial shrinkage characteristics and changes in color and shape of carrots tissues during air drying were studied. Slices dimensions were obtained by computer vision and the color was quantified by chroma, hue, whitening index and total carotenoids contents. The drying time became shorter of 1 h when temperature increased from 60 to 80°C, but sample scorching was observed at 80°C. Blanching pretreatment accelerated the drying process as a result of tissue softening. Two empirical models fitted very well to drying data ($R^2 \geq 0.99525$) and five among reported shrinkage models highly fitted to the data with $R^2 \geq 0.99752$. A new simple model, the Nahimana et al. model gave excellent fit to shrinkage data ($0.99525 \leq R^2 \leq 0.99981$) and was then proposed as an additional shrinkage model. Blanched samples underwent higher radial shrinkage compared to non-blanched; the highest radial shrinkage was $63.49 \pm 4.73\%$. The cortex tissue of fresh and dried carrot samples showed better color than the core due to its higher chroma and lower whitening index. Total carotenoids were also higher in cortex and ranged from 15.80 ± 0.02 to 2.27 ± 0.00 mg/100g sample. Samples' color and main shape descriptors underwent significant changes during drying.

Key words: Carrot, drying, shrinkage, model, shape, color, carotenoid.

INTRODUCTION

The first evidence from writings on red-orange carrots was from the 18th century, while the first accepted evidence of cultivation of modern day carrot came from tenth-century Afghanistan and Iran from where it spread throughout Asia and Europe (Banga, 1957; Baranska et al., 2006). In cross section (Figure 1A), the root mainly consists of an inner xylem (core) surrounded by an outer phloem (cortex). The ratio between cortex and core is an indication of differentiation of carrots, because the fraction of the core decreases during ripening in favor the cortex (Schulz and Köpke, 1992).

Research on carrots is often concerned with its provitamin A content (Metzger et al., 2008) which is associated with reduced lung and breast cancer (Pisani et al., 1986), improved vitamin A concentration,

modulation of the human immune function (Watzl et al., 2003), and increased levels of serum antioxidants (Garcia-Closas et al., 2004). Besides its nutritional carotenoids, sugar, and crude fiber, carrot also contains minerals and other phytochemicals such as phenolics, polyacetylenes, isocoumarins, terpenes and sesquiterpenes.

The changes in fresh food quality during drying vary with the drying method and conditions (Krokida et al., 1998). Some changes, such as the puffing, are desirable (Erle, 2005), but others such as shrinkage, losses in color, shape and nutrients usually lower the quality and reduce consumers' acceptability. Shrinkage is accentuated when conventional drying methods such as air-drying are used than when freeze-drying or microwave drying are employed (Lin et al., 1998). However, due to its cost advantage, air-drying is the most used dehydration method (Górnicki and Kaleta, 2007); it has been extensively studied in carrots' drying (García-Pérez et al., 2009; Romano et al., 2009; Witrowa-Rajchert, 2009).

*Corresponding author. E-mail: min@jiangnan.edu.cn. Tel: +86-510-85919150. Fax: +86-510-85877225.

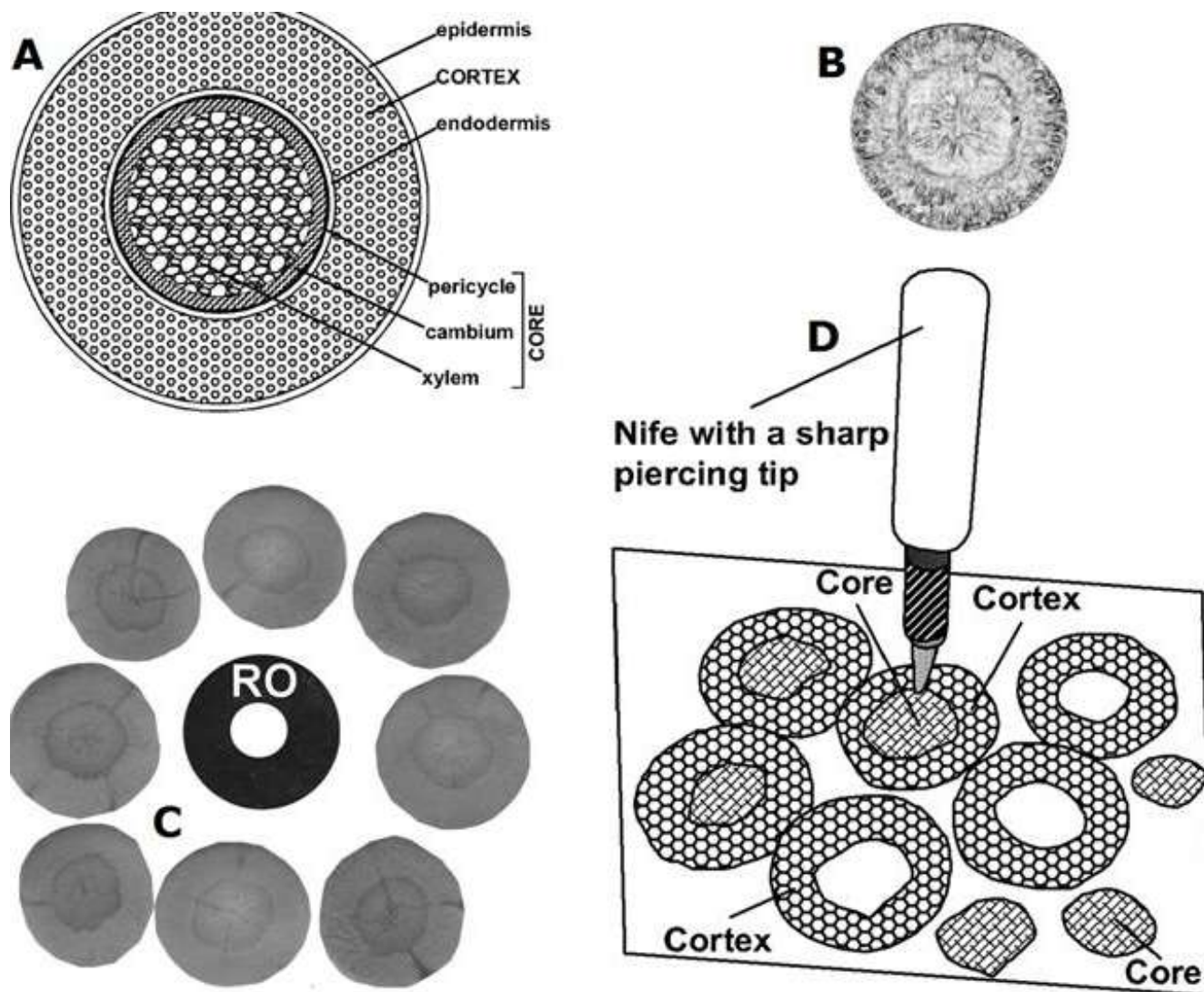


Figure 1. A, Schematic view of carrot tissues on a radial root section; B, clarified boundaries between core and cortex using the software ImageJ; C, arranging slices around a reference object (R.O) prior to image acquisition; D, core-cortex separation along the endodermis of carrot slice.

Carrots discoloration occurs also during air drying. Color loss is due to enzymatic and/or non-enzymatic browning. Food color is due to several pigments such as carotenoids. Many hundreds of carotenoids are found in nature among which β -carotene, lutein, lycopene, β -cryptoxanthin, and α -carotene are the major five (FAO/WHO, 1998). Carrots carotenoids are mainly β -carotene and α -carotene; these are fat-soluble pigments responsible for orange color and capable of conversion into Vitamin A. Scientific literature contains just sparse reports on color differences between the core and the cortex tissues of carrot (Buishand and Gabelman, 1979; Nahimana and Zhang, 2011). The net result of discoloration, shrinkage and shape change is that the consumer would not want to purchase and consume the product. This is to say that the evaluation of these

qualities has a significant meaning to consumers and food producers.

In spite of well known histological differences between core and cortex, there are no reports on tissue specific response during drying. For example, there are no data on how they shrink and lose color, carotenoids or shape during drying. In this study, a computer image analysis method using the software ImageJ (Rasband, 2010) was used to measure accurately samples dimensions. ImageJ has been reported to provide rapid, consistent, and objective measurements for several agricultural products (Igathinathane et al., 2009; Igathinathane et al., 2008; Rodieck, 2008). The objective of this work was to use hot air drying method to dry carrot slices and determine the drying mechanism and radial shrinkage, study and compare the tissue-specific quality changes.

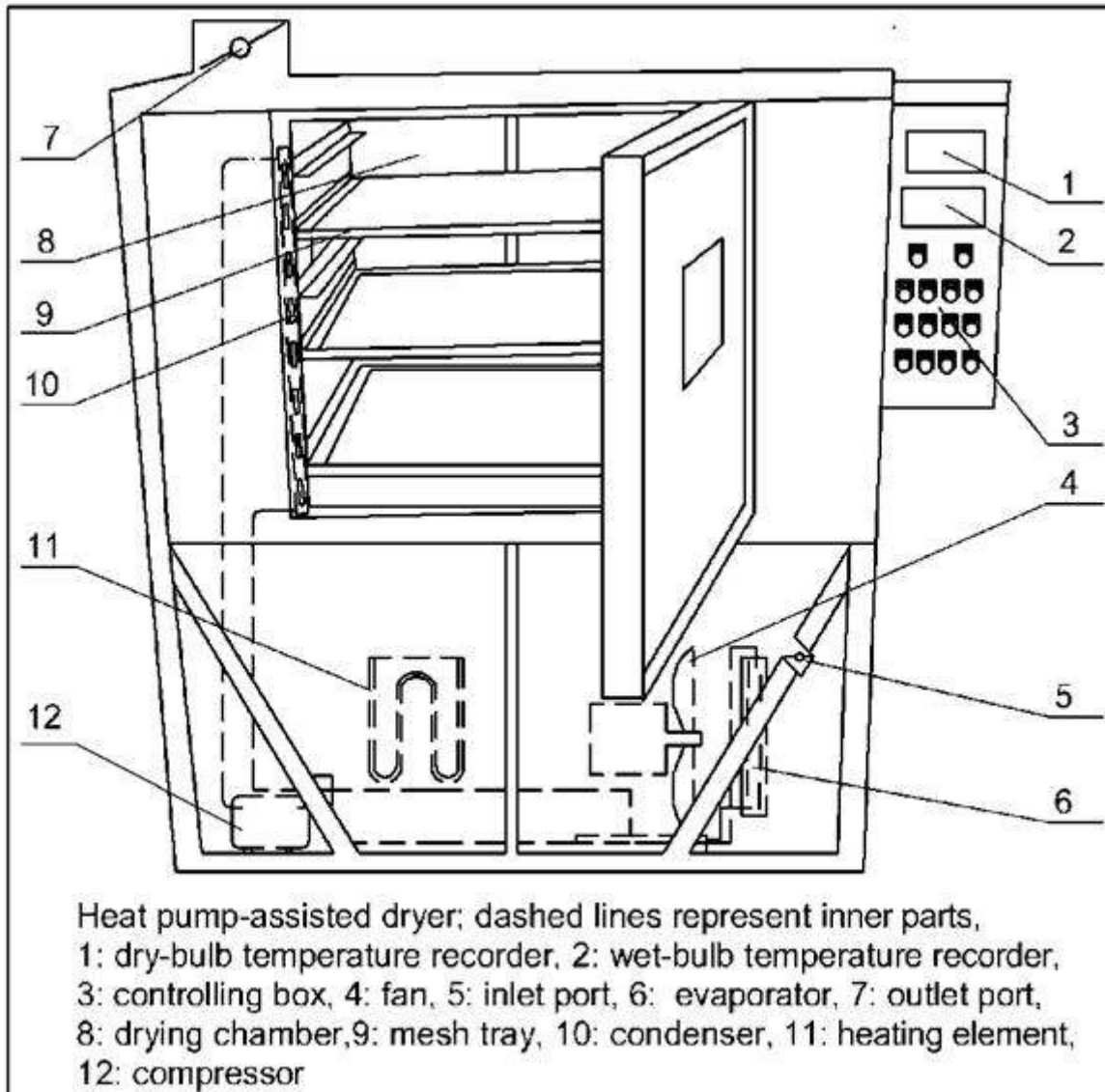


Figure 2. The heat pump-assisted equipment used during drying.

MATERIALS AND METHODS

Drying experiments

Carrots roots were bought from a local market, washed and cleaned. A pre-test experiment was carried out following the Thompson method (Thompson, 1969) to determine roots cylindricality. After washing, carrot roots were peeled and sliced into about 5 mm-thick slices. Blanching of slices was done in hot water at about 90°C for 4 min and was terminated by cooling in running water. Drying experiments were done at two temperature levels (60 and 80°C). The relative humidity and air speed in the dryer were about 30% and 1.5 m/s, respectively. A heat pump hot air dryer (HPD) (Sunny Trade Co., Shanghai, China) was used for these experiments (Figure 2). The main advantages of using HP are its energy saving potential and the ability to control drying temperature and air humidity.

The HPD was a combination of two sub-systems: a heat pump and a dryer. The refrigerant at low pressure is vapourized in the

evaporator (Figure 2, 6) by heat drawn from the dryer exhaust air. The compressor (12) raises the enthalpy of the working fluid of the heat pump and discharges it as superheated vapour at a higher pressure. Heat is removed from the working fluid and returned to the process air at the condenser (10). The refrigerant is then throttled to the low-pressure line using an expansion valve and enters the evaporator to complete the cycle. In the dryer system, hot and dry air at the exit of the condenser is allowed to pass through the drying chamber (8) where it gains latent heat from the material. The humid air at the dryer exit then passes through the evaporator where condensation of moisture occurs as the air falls below the dew point temperature.

Water content and drying curves

The water content on the wet basis (wb) for fresh carrot samples was determined gravimetrically by oven drying method in three

replicates and calculated as shown in Equation 2. For the dry samples, the water content was determined on the dry basis (db) following Equation 3. The conversion of moisture content from wet to dry basis was done by dividing the wet basis water content by the dry matter factor; the percentage of the dry matter expressed as a decimal.

$$\text{Wet basis water content (\%)} = \left(\frac{M_{\text{initial}} - M_{\text{dried}}}{M_{\text{initial}}} \right) \times 100 \quad 1$$

$$\text{Dry basis water content (g/g dry solids)} = \left(\frac{M_{\text{initial}} - M_{\text{dried}}}{M_{\text{dried}}} \right) \quad 2$$

Where, M_{initial} is the mass of sample before drying and M_{dried} is the mass of completely dehydrated sample by oven method. The drying curves were obtained by plotting the instant moisture contents (on dry basis) versus drying time. Partial regressions were performed on the drying data in order to characterize the drying mechanism.

Fitting drying curves data to different models

Normalized drying curves were obtained following the method of Van Meel (1958), by plotting moisture ratio vs. drying time; the moisture ratio was given by the relation:

$$\text{Moisture ratio} = \frac{X - X_e}{X_0 - X_e} \quad 3$$

Where, X_0 represented initial moisture content, X and X_e were instant and equilibrium moisture contents (g H₂O/g dry solids). The fitting trends of 13 empirical drying models reported in literature were analyzed but only two of them, the Aghabashlo model (Aghabashlo et al., 2008) and the Wang and Singh model (Ozdemir and Devres, 1999) shown in Equations 4 and 5; were reported due to their high goodness of fit.

$$\text{Moisture ratio} = \exp\left(-\frac{k_1 t}{1 + k_2 t}\right) \quad 4$$

$$\text{Moisture ratio} = 1 + at + bt^2 \quad 5$$

Where, k_1 , k_2 , a and b are models' parameters and t is the drying time. The software Datafit version 9.0.59 (Oakdale Engineering, Oakdale 15071, USA) was used for the fitting processes. The coefficient of multiple determinations (R^2) and the standard error of estimate were the main criteria for judging the model's suitability to drying data; however other statistical parameters (not reported) such as the residuals scattering pattern and their probability were considered during fitting. The different models' parameter values and other fitting statistics were obtained using the software Datafit.

Samples image acquisition

A CCD digital camera (Samsung i85) equipped with an LCD display, optical zoom and a high-resolution of 8.2-megapixels was used. During image acquisition, carrot slices and/or roots were

captured together with reference object (RO) of known dimensions serving in units' conversion from pixels to real dimension units (Figure 1C). Both the object and samples were laid on a flat surface and the camera was centrally focused on them as shown in the Figure. In case of root length measurement, a ruler of known length was used as reference object.

Sample dimensions and shape

Digital images were copied to a computer and their dimensions measured using the software ImageJ version 1.43 q (Rasband, 2010). For root dimensions measurement, a given reference length served in converting the digital unit (i.e., pixels) images into centimeters; in case of surface area of slice base, the conversion was done by using the known diameter of the image of the standard object simulating slices (Figure 1C). Since the slices were very thin, two dimension shape descriptors were considered which were circularity, aspect ratio, roundness, solidity, minor axis and major axis; defined in equations 6 to 9.

$$\text{Circularity} = \frac{4\pi \times \text{Area}}{\sqrt{\text{Perimeter}}} \quad 6$$

$$\text{Roundness} = \frac{4 \times \text{Area}}{\pi \times \sqrt{\text{Major axis}}} \quad 7$$

$$\text{Solidity} = \frac{\text{Area}}{\text{Convex area}} \quad 8$$

$$\text{Aspect ratio} = \frac{\text{Major axis}}{\text{minor axis}} \quad 9$$

Radial shrinkage

The radial shrinkage of carrot slices was done using the method of Singh et al. (2007) and approximated by the percent change of the slice equivalent radius (ER). The term *equivalent* was introduced because carrot slices were not perfectly circular as shown in Figure 1C (a perfect circular slice would look like that schematized in Figure 1A). ER was defined as the radius of a perfectly circular slice of the same base area as that of the corresponding slice. Radial shrinkage during drying for the core and cortex tissues was calculated as:

$$\text{Radial shrinkage (\%)} = \left[1 - \left(\frac{ER}{ER_0} \right) \right] \times 100 \quad 10$$

Where, ER and ER₀ represent respectively, the instant and initial equivalent slice radii. ER values of eight slices were obtained for each experiment and their means reported. Each lot could be removed from the dryer and photographed to make digital stock samples from which the base area was obtained. The time elapsed between removing and returning samples into the dryer was sufficiently short to have negligible effect due to process interruption.

Modeling radial shrinkage

Five empirical models currently reported to fit shrinkage data of agricultural commodities were fitted to the experimental data. These were the Adapted Lozano-1, the Adapted Lozano-2, the Correa et al. model, the Togrul and Inspir model and the Adapted Bala & Woods model shown in Equations 11 to 15 respectively. Their corresponding biography is found in Nahimana et al. (2011). In addition, a new shrinkage model, named the 'Nahimana et al. model' (Equation 16) was tested if it fits into category of already reported models that predict shrinkage. A non-linear regression analysis by the Least Square method was conducted using the software Datafit to fit these models to experimental data. Again R square and the standard error of estimate were the primary criteria. However, due to the extremely large data, only the Nahimana et al. model was reported in details, while for others just R square was reported. The model parameters were determined at a confidence level of 0.95.

$$\frac{ER}{ER_0} = a + b \frac{X}{X_0} + c \exp\left(\frac{d}{X+e}\right) + \left(f + \frac{g}{X_0+h}\right) \left(1 - \frac{X}{X_0}\right) \quad 11$$

$$\frac{ER}{ER_0} = a + b \frac{X}{X_0} + c \exp\left(\frac{d}{X_0}\right) \quad 12$$

$$\frac{ER}{ER_0} = \frac{1}{a + b e^X} \quad 13$$

$$\frac{ER}{ER_0} = a + b \exp(cX) + d \exp(eX^f) \quad 14$$

$$\frac{ER}{ER_0} = 1 - a \left(1 - \exp(b(X - X_0))\right) \quad 15$$

$$\frac{ER}{ER_0} = a - b c^X \quad 16$$

Where ER and ER_0 are, respectively, the instant and initial slice radius; X and X_0 are the instant and initial water contents (db) and the letters a to h are models parameters.

Samples microstructure and image before and after drying

Fresh and hot air dried carrot slices were involved in these experiments. The microstructure was determined using the scanning electron micrograph (SEM). In samples preparation for SEM, samples were fixed in 0.1% glutaraldehyde in 0.1 M phosphate buffer (pH 7.2) for 2.5 h at room temperature. After this, the conductive staining by osmium tetroxide was applied on them; the samples were then subjected to dehydration in graded series of ethanol (30, 50, 70 and 90%). Using critical point drying, the samples were then totally dehydrated, and at last the gold coating on samples was done through ion sputtering. Prior to microstructure visualization, gold coated samples were fixed on brass holders with silver paint mounted on the sample holder into the specimen

chamber of a SEM equipment (Quanta200, FEI Co., Holland) and the electron scanning imaging was performed on samples. The samples' digital micrographs were then saved to the computer for further analysis and interpretation of their microstructure.

The changes in sample dimensions and shape during drying were pictorially visualized by photographing the slices arranged around a reference object (RO) of 4 cm in diameter (Figure 6). Each slice position before drying was numbered and kept unchanged during the whole process of drying and taking photographs.

Color measurement

The dehydrated product was ground using the blender/food processor (Keshun JH380-A Guangdong, Shanghai) for 4 min and the powder transferred in transparent cuvettes in four replicates. The color was evaluated using a Konica Minolta Model CR-400/410 colorimeter. Readings were expressed in $CIE1976 L^*a^*b^*$ scale, where L^* measures lightness; a^* represents greenness to redness and b^* represents blueness to yellowness. The total color difference (ΔE^*), chromaticity difference (ΔC^*), hue angle (H°) and the coefficients of variation (CV) for a^* and b^* (Equations 17 and 20), were used for quantifying color changes upon drying. Fresh carrot slices were used as control samples. The discoloration of the samples' surface during drying was quantified by the whiteness index (WI) values, calculated by the Equation 21.

$$\Delta E = \sqrt{(\Delta L^*)^2 + (\Delta a^*)^2 + (\Delta b^*)^2} \quad 17$$

$$\Delta C = \sqrt{(\Delta a^*)^2 + (\Delta b^*)^2} \quad 18$$

$$H^\circ = \arctan\left(\frac{b^*}{a^*}\right) \quad 19$$

$$CV(\%) = \frac{\sigma}{X} \times 100 \quad 20$$

$$WI = 100 - [(100 - L^*)^2 + a^{*2} + b^{*2}]^{\frac{1}{2}} \quad 21$$

Here X is the average value for a^* and b^* and σ their standard deviation; ΔL^* , Δa^* and Δb^* are differences in L^* , a^* and b^* between control and dried samples; WI is the whiteness index.

Determination of total carotenoid contents

The total carotenoid contents in fresh samples, in dry samples and in the two main carrot tissues were determined by spectrophotometric method. Their extraction from different tissues was done following the method of Rangana (1977). A random sampling was performed by blind drawings of dried slices from the stock. If dried alone the tissues were used directly; in case of the whole slice, tissues were separated along the endodermis; while in case of fresh samples, carrot roots were first peeled before slicing and sampling.

A representative sample of known mass containing 10 to 500 μg of carotenoids was repeatedly extracted by grinding in a mortar containing a mixture cold acetone and Kieselgur. The extraction stopped when the residue became colorless. After filtration, the

acetone-carotenoid mixture was transferred to a separating funnel and a volume of petroleum ether slightly greater or equal to that of the mixture was added to it. Water was gently added to it in order to drain out acetone and transfer the carotenoids into petroleum ether. The petroleum ether mixture was dried with anhydrous sodium sulfate to remove all residual moisture. Finally proper dilutions of carotenoids solutions were performed prior to measurements of their concentrations using the UV/VIS 2600 Spectrophotometer. Petroleum ether was used as blank; the absorbencies were read in three replicates at 452 nm and three repetitions were done for each. The calculations of total carotenoids contents were done by comparing their absorptions to those of the standard curve as shown in Equation 22. The standard curve was built by performing serial dilutions in petroleum ether, of 99.7% pure β -carotene purchased from Sigma and plotting the dilutions concentrations vs. their corresponding absorbencies. A linear curve with a high coefficient of determination ($R^2=0.999$) and equation $y = 0.262x + 0.038$ was obtained.

$$\text{carotenoids contents} \left(\frac{\text{mg}}{100\text{g}} \right) = \frac{\frac{\mu\text{g of caroten/ml}}{\text{as read from the curve}} \times \text{Dilution factor} \times 100}{\text{Weight of sample} \times 1000} \quad 22$$

Statistical analysis

The statistical analysis of the experimental results was done using the software SPSS version 11.5. One way analysis of variance (ANOVA) and Duncan-multiple-range test were used to test both hypothesis and significance in samples' mean differences. The data significance level was set at 95%. The correlation coefficient between data sets was determined by Pearson's correlation procedure. A principal component analysis was applied to slices shape data and to assess the main shape descriptors by considering the Eigenvalues of different shapes. The software Datafit version 9.0.59 was used to output the statistical values of model parameters used during modeling drying and shrinkage data.

RESULTS AND DISCUSSION

Water content

The oven drying method was used to determine the percent water content (on the fresh basis) of the fresh cut blanched and unblanched carrots. For the fresh carrots, the water content (wet basis) was slightly higher in the blanching-pretreated samples compared to the unblanched samples (92.28 vs. 90.34%). The difference is explained by possible moisture uptake during blanching or tissue softening during this process, making the moisture to be removed at a higher extent during oven drying; while the unblanched samples kept their firm structure that limits the extent of moisture removal. Earlier works (Smith et al., 2007) indicated that approximately 90% of the weight of fresh carrot is due to water, which agrees with our results. Blanching with hot water was reported to cause increase in bulk density and cause structural collapse in tissues (Maté et al., 1999). So blanched and non-blanched tissues could be expected to respond differently to the drying process, resulting for example in different equilibrium moisture

contents, different drying curves and rates or give different quality dried products. The final moisture contents (wet basis) in dry products were 10.23, 10.57, 13.10 and 9.82%, for the unblanched samples dried at 60°C (ud60), the blanched samples dried at 60°C (bd60), the unblanched samples dried at 80°C (ud80) and the blanched samples dried at 80°C (bd80) respectively.

Drying curves and their suitable models

The moisture degradation during drying is shown in Figure 3. Due to more heat energy, drying at 80°C shortened the drying time by 60 min, making it to pass from 300 min at 60°C to 240 min at 80°C. At same drying temperature, initial moisture content on dry basis was higher for blanching-pretreated samples compared to non-pretreated. This resulted from the soft tissue generated by blanching which caused higher moisture removal during oven determination. This means that lower dry solids mass was yielded, causing increases in calculated water content. For instance, initial fresh sample weights of 108.283 and 109.700 g for the runs ud60 and bd60 respectively, became equilibrated at 11.656 and 9.469 g at the end of drying. The equilibrium moisture contents (dry basis) for ud60, bd60, ud80 and bd80, were respectively 11.39, 11.83, 15.07 and 10.89%; corresponding to wet basis moisture contents of 10.23, 10.57, 13.10 and 9.82%, respectively. Up to the half drying time instant moisture contents were affected by sample pretreatment; being highest for blanching-pretreated compared to non-pretreated samples. In addition, greater amounts of free moisture were removed during these first half-drying periods compared to the second half period. For instance the first half-time drying at 60°C (which was 150 min) removed 84.90 and 84.60% of total free moisture for ud60 and bd60, respectively; while at 80°C, the first half-time drying period (which was 120 min) took out 91.13 and 90.15% of total free moisture for the Runs ud80 and bd80, respectively. Furthermore a good linear relation existed between water content and drying time in the whole first half-drying time period. This was confirmed by high coefficients of determination (R^2) and low standards errors of estimates. R^2 for ud60, bd60, ud80 and bd80, were respectively 0.99151, 0.99474, 0.98639 and 0.99042; their corresponding standard errors of estimates were 0.31039, 0.30959, 0.50346 and 0.54958. From this relation it is deduced that in the whole first half-drying period, carrots tissues underwent a predominant external moisture removal process; while in the second half, a shift in the internal moisture transport occurred. This continued until it entered the tailing period where the drying process removed little moisture due to greater resistances to mass transfer generated by such factors as high density in internal tissue network, structural collapse by shrinkage, case hardening, etc.

From the slopes of regression lines on Figure 3, it can be deduced that mean drying rate was affected by drying

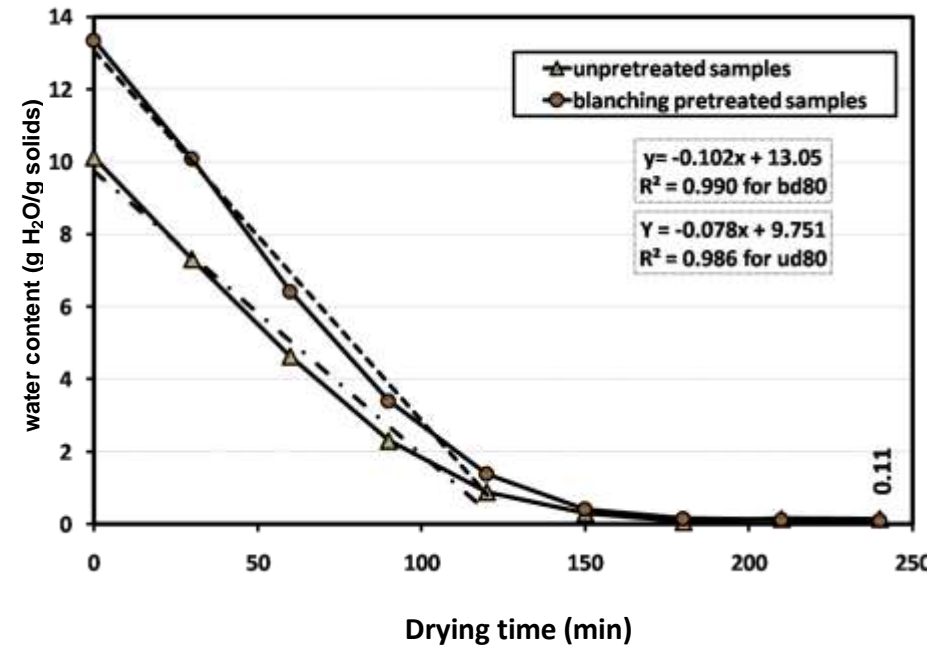
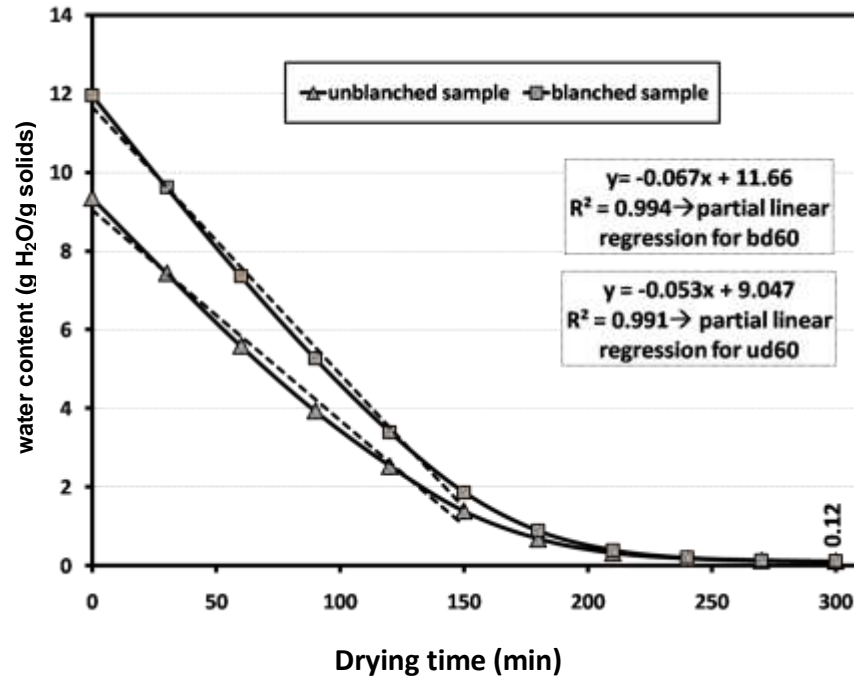


Figure 3. Water content of carrot samples as influenced by pretreatment method, drying time and temperature; bd60/bd80: blanched samples dried at 60/80°C, ud60/80: unblanched samples dried at 60/80°C.

conditions; for ud60, bd60, ud80 and bd80, drying rate were 53, 67, 78 and 102 g of water removed per kg dry solids per minute respectively. It is currently reported (Prabhanjan et al., 1995) that high moisture foods are susceptible to exhibit periods of constant drying rates; in accord with our results of the first half drying time period. The drying rates were proportional to instant moisture contents. Blanching pretreatment and higher drying temperatures increased the drying rates tremendously especially in earlier drying stages.

Of the 13 empirical drying models tested, only two models, the Agabashlo model and the Wang and Singh model, fitted to drying data very well. The popularly used Page model and many models

just resulted in very low R^2 values (≤ 0.5) while the two suitable models recorded R^2 greater than 0.99 and very low standard errors of estimates (Table 1). Furthermore Figure 4 shows that the modeled data were very closely scattered near the experimental data, revealing that these models can confidently be used to predict instant moisture contents of carrot during drying.

Radial shrinkage

The radial shrinkage expressed as percent changes of the equivalent radius (ER) of carrot slices, was studied and the results are shown in

Figure 5. As shown in Figure 6, hot air drying caused the slices to undergo very high radial shrinkage. For instance, considering the Run ud60 (Figures 5 and 6), the mean initial ER values for cortex and core of the eight slices were respectively 2.24 ± 0.07 and 1.34 ± 0.07 cm. At half-drying time, these values decreased to 1.34 ± 0.17 and 0.75 ± 0.14 cm; and at the end, ER for dried slices were 0.92 ± 0.13 and 0.49 ± 0.07 cm. As shown in Figure 5, the above ud60-ER values at half-drying time corresponded to radial shrinkage of 39.99 ± 7.97 and $43.56 \pm 11.88\%$ for cortex and core respectively; while in the end, they turned to final shrinkage of 58.82 ± 5.11 and $63.41 \pm 5.31\%$ for cortex and core respectively.

Table 1. Drying models parameters and their statistical values.

Sample	Model	Parameter	Value ± STD at 95% confidence level	R ²	Standard error of estimate
bd60	Agabashlo	k ₁	0.00668±0.00014	0.99992	0.00335
		k ₂	-0.00311±0.00010		
ud60	Agabashlo	k ₁	0.00717±0.00014	0.99993	0.00323
		k ₂	-0.00298±0.00010		
bd60	Wang and Singh	a	-0.00776±0.00027	0.99792	0.01718
		b	0.00001±0.00000		
ud60	Wang and Singh	a	-0.00794±0.00022	0.99848	0.01454
		b	0.00002±0.00000		
bd80	Wang and Singh	a	-0.01048±0.00061	0.99525	0.02748
ud80	Wang and Singh	a	-0.01095±0.00060	0.99542	0.02674

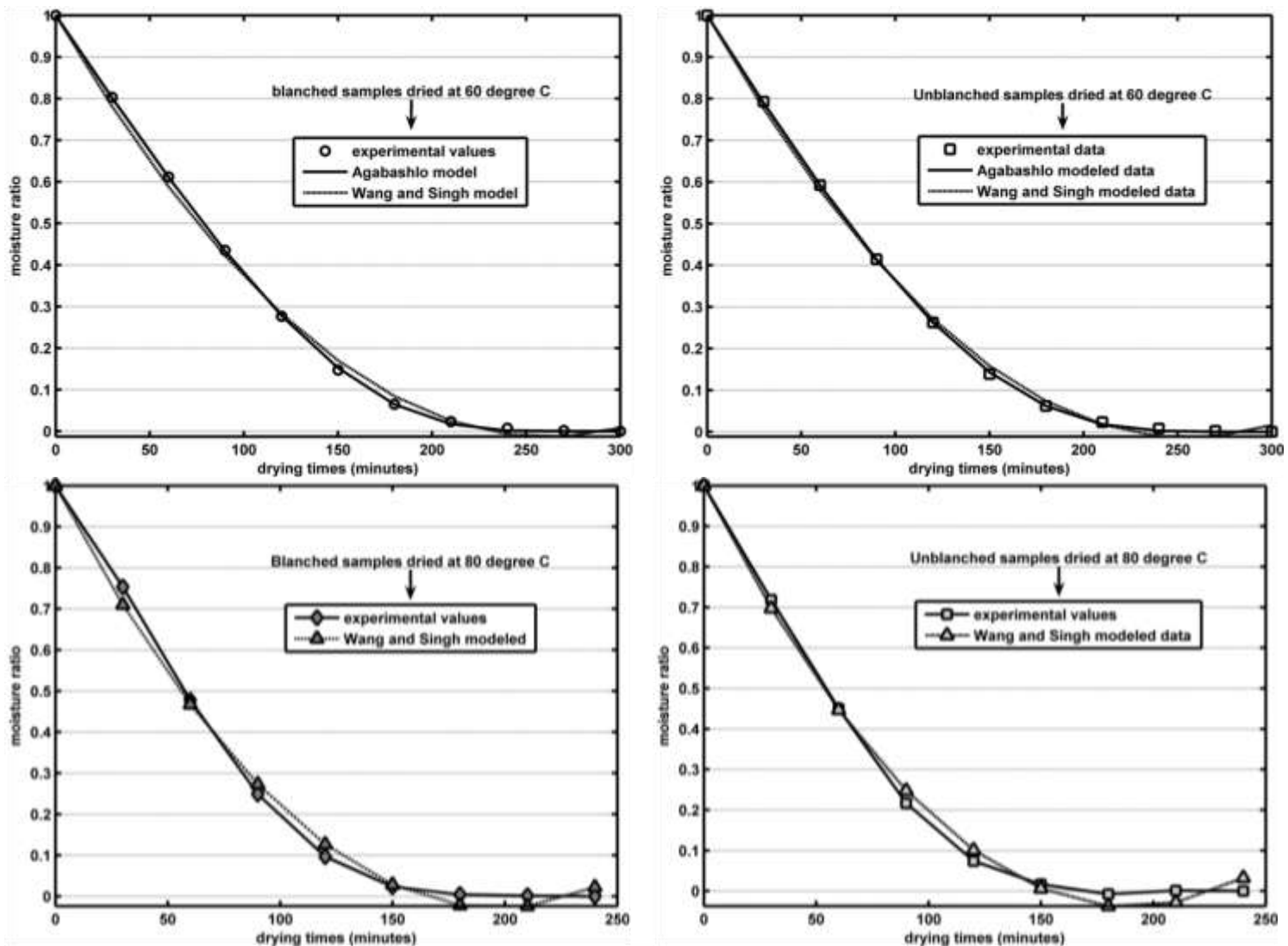


Figure 4. Graphical fitting trends of different drying models to experimental data.

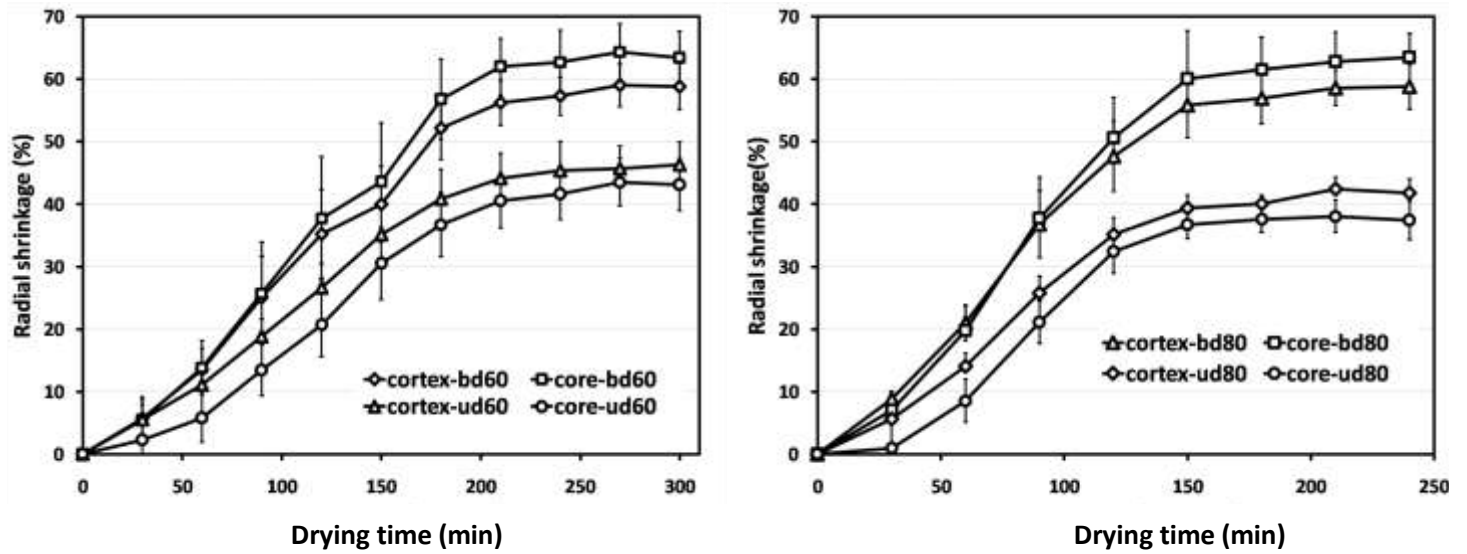


Figure 5. Radial shrinkage vs. drying time for core and cortex of carrot slices at different drying conditions.

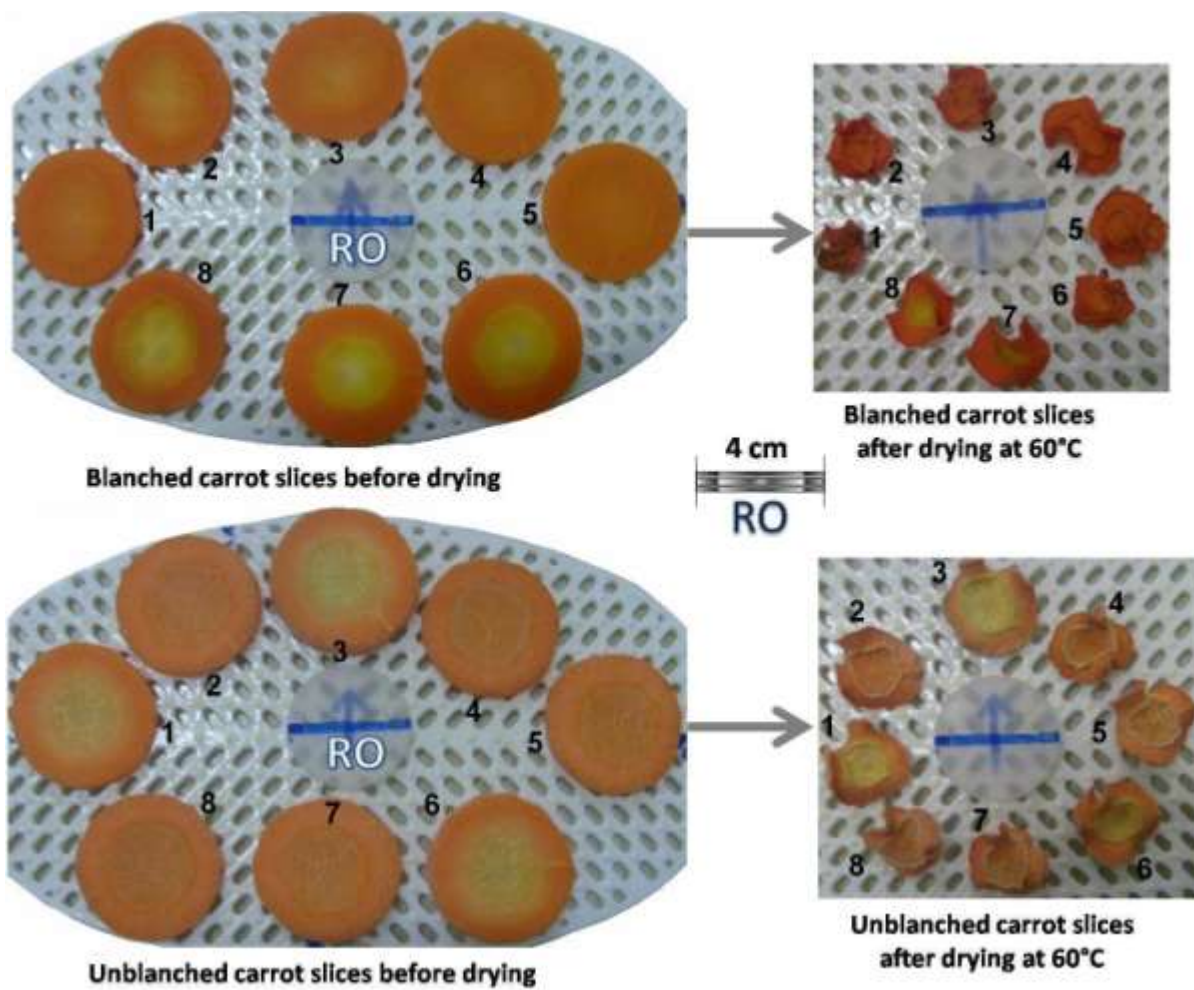


Figure 6. Photographic images of blanched and unblanched carrot slices before and after drying at 60°C, RO is the reference object (of 4 cm in diameter) that served in scaling each image size, the same slice numbering designate the same slice before and after drying.

The run ud80 also exhibited higher shrinkage in cortex than in core. These results reveal that radial shrinkage was not the same for the two tissues. Shrinkage was influenced by the drying conditions and pretreatment. Figure 5 shows that increasing the drying temperature from 60 to 80°C caused a mean decrease in radial shrinkage of about $5.12 \pm 0.85\%$ for dried non-pretreated carrot slices. In all cases, blanched samples recorded higher shrinkage values than non-pretreated samples dried at same temperature. In addition, blanching-pretreatment seemed to remove the shrinkage differences between core and cortex and/or even invert ranking order of their shrinkage values. This was particularly observed with the Run bd80, where its core recorded higher values than its cortex (that is; $63.49 \pm 4.73\%$ vs. $58.76 \pm 4.73\%$), which was an inverse situation of what resulted from drying non-blanched samples at either 60 or 80°C. The run bd60 made an exception where core and cortex recorded insignificant shrinkage differences.

Shrinkage is moisture dependent. As moisture is removed from tissues pressure imbalance is created between the inside and outside of tissue, generating compressive stresses that lead to greater shrinkage. The fact that for unblanched samples the radial shrinkage of the cortex was higher than that of the core could imply different rates in moisture removal between the two tissues, resulting from their texture and microstructure differences. It was reported that the core is mainly vascular, although containing a few cortex-type cells radially arranged around its tracheary elements (Smith et al., 2007). Cortex, on the other hand, is a parenchymatic storage tissue with more flexible cells than those of core; this offers less rigid structure that would reduce the collapsing phenomena upon shrinkage. Blanching changes the shrinkage predictability in the two tissues because the heat provided by the boiling liquid during blanching penetrates within the tissues, destroying their structure and texture. Blanched samples recorded higher shrinkage values due to soft texture and less resistance to mass transfer during drying. As in case of the drying mechanism discussed in section 3.2, most shrinkage occurred in the first half-drying time period, where its mean value at 80°C was $82.92 \pm 3.11\%$, with a minimum of 79.72 and a maximum of 86.66%; at 60°C, the shrinkage mean value was $70.86 \pm 3.58\%$ with a minimum of 67.99 and a maximum of 75.91%. Thus, the second drying period was characterized by a shrinkage tailing pattern since there were no more considerable radius changes occurring. From these results, it can be formulated that during hot air drying of carrot slices, if optimum qualities of the dried material are required, a particular attention should be fixed on drying period, mainly the two half drying time periods. We have shown that most of moisture removal and shrinkage happen in the first drying period, leaving the second period with minimum contributions to these phenomena. Therefore it is reasonable to conclude that the quality degradation for

carrots during drying deepens in the second period, since there is no enough moisture to protect the heat sensitive compounds and/or other nutrients. As the drying food material collapses due to shrinkage, its shape is also destroyed because anisotropic shrinkage is what happens in many cases of food dehydration. This led to the need of quantifying the shape changes during drying.

Modeling radial shrinkage

To our knowledge, prior to this report, there were no previous works on radial shrinkage of carrot slices during hot air drying. Hence, it seemed reasonable to study how our experimental data could be predicted by the mathematical shrinkage models reported in literature. As shown in Equations 11 to 15, five existing models were analyzed; and a new model, called the Nahimana et al. model (Equation 16) was evaluated to see if it could fit in the category of shrinkage models. The results for the new model were reported in details in Table 2 and for other models; R^2 and the standard error of estimates were provided in Table 3. In addition, model fitting trends to data were graphically shown in Figures 7 and 8. The analysis of variance (ANOVA) showed that all the models were significant at a confidence level of 95%, R^2 values were very high and the standard errors of estimate were very low. Table 2 shows that for the Nahimana et al. model, R^2 varied from highest, 0.99981 (for ud60-cortex) to lowest, 0.99525 (for bd60-cortex), and the standard error of estimate varied from 0.00270 (for ud60-cortex) to 0.01730 (for bd60-cortex). All other samples values ranged between those extreme values. A significant ($p \leq 0.01$) Pearson correlation of 0.87 existed between R^2 and standard errors of estimate, where lowest errors were related to highest R^2 values. The fitting process of models reported in literature also yielded to very high R^2 values (Table 3), varying from the highest (0.99986) for Adapted Lozano-1(ud60-cortex) to the lowest (0.99252) for Correa et al. (bd60-cortex). These results led to a conclusion that all the tested models were statistically suitable to predict experimental data. Figures 7 and 8 also supported this idea as they exhibited close dispersions of experimental data around modeled curves. Thus, the Nahimana et al. model is proposed as a new model predicting with very high confidence, the experimental data of radial shrinkage during hot air drying of carrots. However future research on its fitting trends to other agricultural commodities should be done.

Changes in carrot microstructure during drying

SEM method was used to evaluate the microstructure of outer surface of carrot slices before and after drying at 60°C. Figure 9 shows that good SEM micrographs were obtained since they had good sharpness, is noiseless

Table 2. Parameters of the new shrinkage model (Nahimana et al.) and their statistics.

Sample	Parameter	Value \pm STD at 95% confidence level	R ²	Standard error of estimate
cortex of bd60	a	1.20343 \pm 0.16947	0.99525	0.01730
	b	0.79766 \pm 0.16174		
	c	0.89189 \pm 0.03811		
core of bd60	a	1.19061 \pm 0.14316	0.99614	0.01718
	b	0.84127 \pm 0.13579		
	c	0.88220 \pm 0.03465		
cortex of ud60	a	1.12774 \pm 0.02192	0.99981	0.00270
	b	0.59958 \pm 0.02071		
	c	0.84946 \pm 0.00942		
core of ud60	a	1.05004 \pm 0.02371	0.998979	0.00620
	b	0.49680 \pm 0.02189		
	c	0.77350 \pm 0.02306		
cortex of bd80	a	1.21380 \pm 0.08874	0.999244	0.00728
	b	0.80363 \pm 0.08552		
	c	0.90636 \pm 0.01717		
core of bd80	a	1.15363 \pm 0.05925	0.999361	0.00740
	b	0.79262 \pm 0.05639		
	c	0.88323 \pm 0.01620		
cortex of ud80	a	1.09365 \pm 0.07362	0.997523	0.00953
	b	0.51778 \pm 0.06974		
	c	0.84426 \pm 0.04085		
core of ud80	a	1.05248 \pm 0.05502	0.995526	0.01260
	b	0.44798 \pm 0.05154		
	c	0.78577 \pm 0.05825		

Table 3. Coefficients of multiple determinations (R²) for the shrinkage models reported in literature and applied in this research.

Carrot tissue	Model type	R ²	Carrot tissue	Model type	R ²
cortex of bd60	Adapted Lozano-1	0.99582	cortex of bd80	Adapted Lozano-1	0.99931
	Adapted Lozano-2	0.99373		Adapted Lozano-2	0.99373
	Correa et al.	0.99252		Correa et al.	0.99765
core of bd60	Adapted Lozano-1	0.99623	core of bd80	Adapted Lozano-1	0.99938
	Adapted Lozano-2	0.99474		Adapted Lozano-2	0.99840
	Correa et al.	0.99310		Correa et al.	0.99817
cortex of ud60	Adapted Lozano-1	0.99986	cortex of ud80	Adapted Bala and Woods	0.99752
	Adapted Lozano-2	0.99804		Adapted Lozano-1	0.99757
	Correa et al.	0.99909		Adapted Lozano-2	0.99605
	Togrul and Inspir	0.99971		Correa et al.	0.99729
core of ud60	Adapted Lozano-1	0.99934	core of ud80	Adapted Lozano-1	0.99962
	Adapted Lozano-2	0.99633		Adapted Lozano-2	0.99875
	Correa et al.	0.99921		Correa et al.	0.99786
	Togrul and Inspir	0.99875			

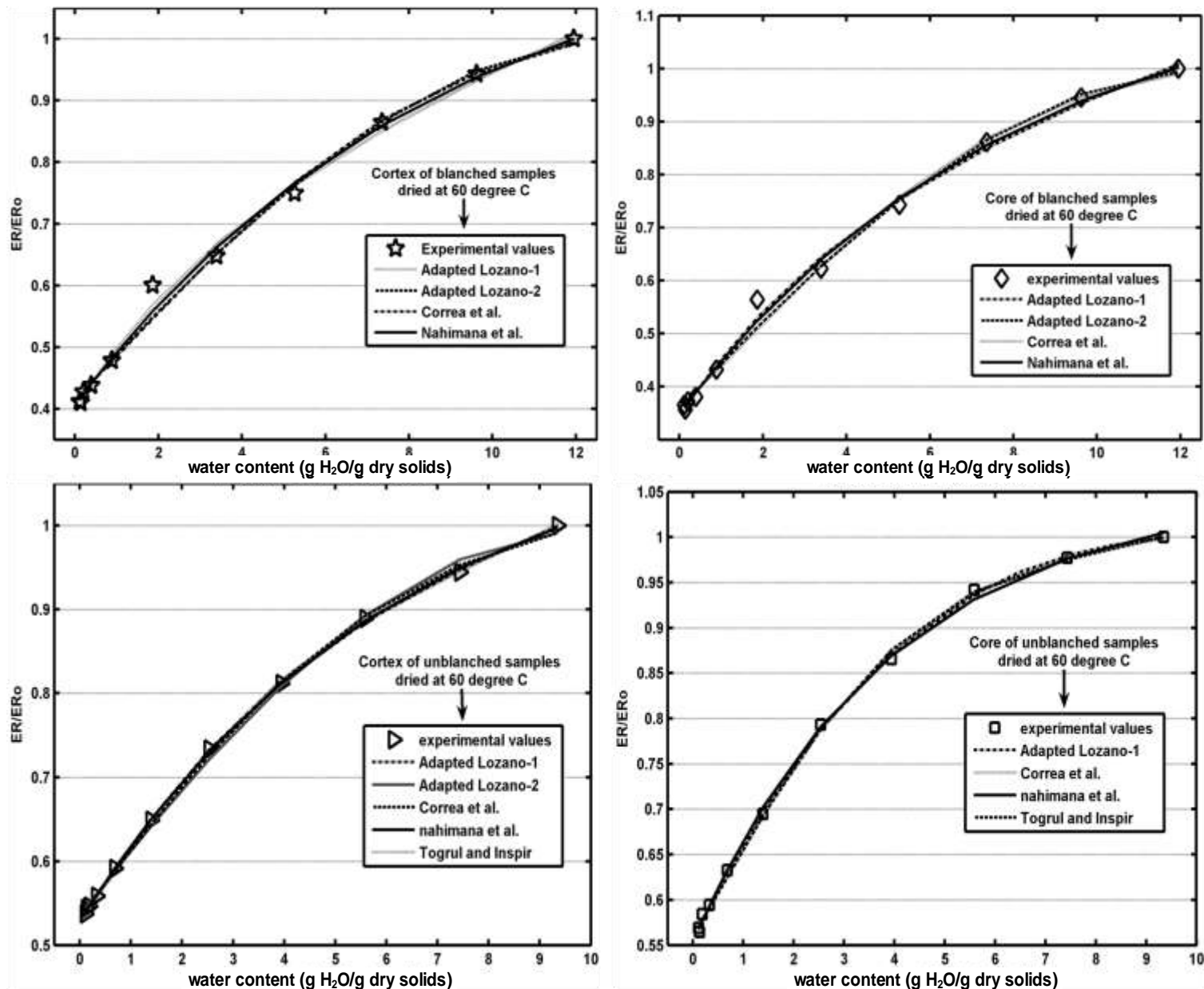


Figure 7. Fitting curves of different models to shrinkage experimental data of samples dried at 60°C

and had optimum contrast and brightness. Furthermore, the microstructural differences between core and cortex in fresh (F-CR and F-CX) and hot air dried samples at 60°C (UD60-CR and UD60-CX) are exhibited by these micrographs. In fresh carrots, though there was clear cell delimitations by cell walls in both tissues, SEM images showed that the cortex is mainly composed of parenchymatous cells (a) among which are dispersed very few xylem-type cells (b), which in fact are images of secondary roots of carrot. On the other hand, the core tissue was mainly represented with xylem tracheary elements (c) and very few cortex-type cells around xylem trachea (d). Unlike fresh carrots where intact tissue

structure was shown, hot air dried carrot slices exhibited a highly dense and collapsed structure, as was reported by Smith et al. (2007). This cellular damage was due to shrinkage during drying. Unlike UD60-CX where at least few recognizable cell structures could still be hardly observed, UD60-CR underwent complete structural collapse during drying, confirming its higher shrinkage values as earlier discussed. For both tissues, the deformation of slice surface was very high during hot air drying. Figure 9 shows that not only does SEM micrographs of dried samples had a collapsed structure, but also had unleavened topographic surface morphology, unlike in the case of fresh slices where fine structured planar surface

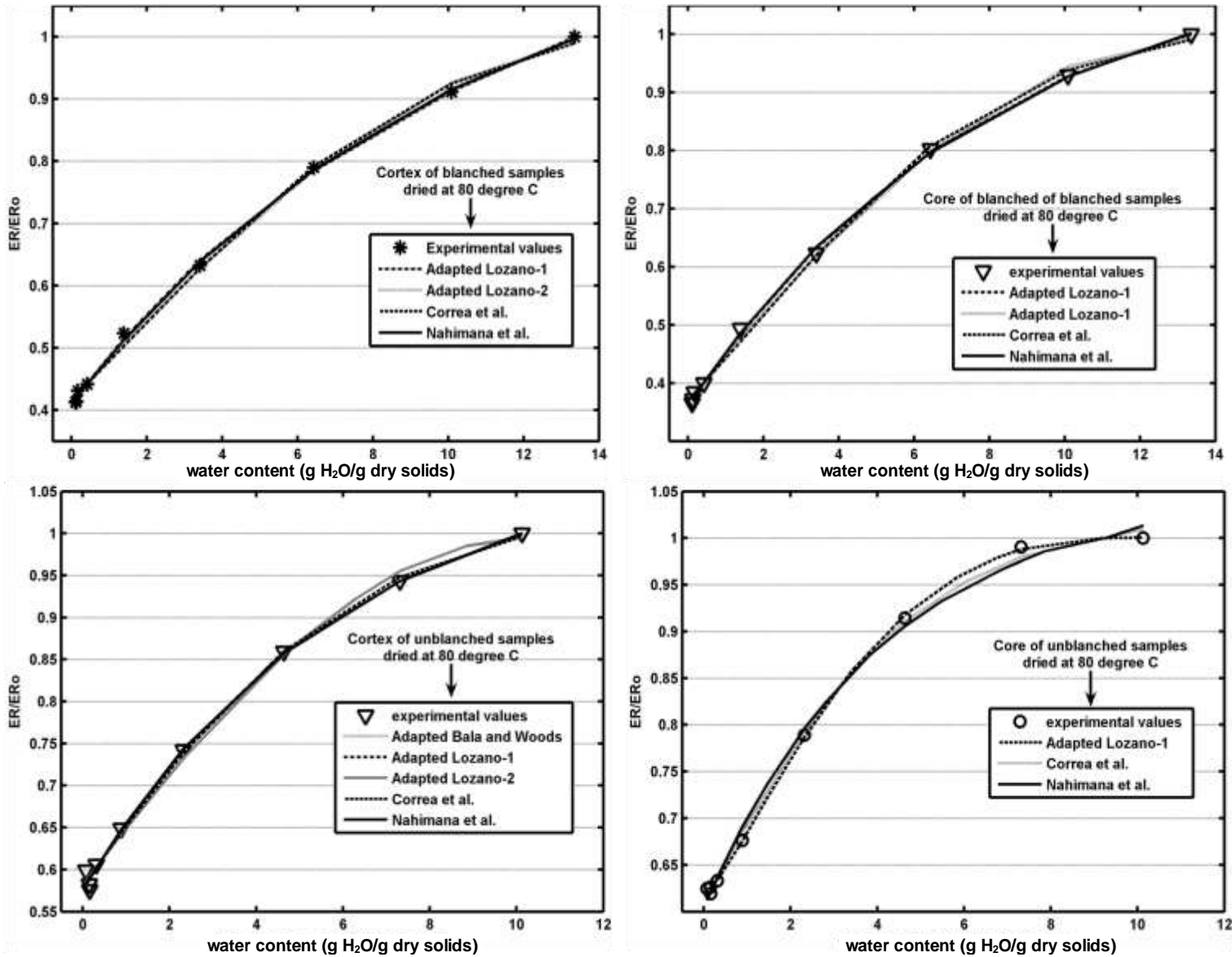


Figure 8. Fitting curves of different models to shrinkage experimental data of samples dried at $80^\circ C$.

was revealed.

Shape descriptors

The food may become non-merchantable if severe shape loss occurs during processing. This happened in our preliminary experiment (results not shown) on hot air drying of carrot cubes. When sensory members were asked to guess, majority failed to identify the initial cubic shape of dried samples. For fresh-cut carrots, the shape cylindricality of roots frequently sold on the market was measured and found varying from 0.37 ± 0.01 to 0.71 ± 0.01 . Most of our drying experiments utilized the roots with high cylindricality (that is, closer to 0.71 ± 0.01). For

fresh and dried carrot slices, six shape descriptors were first considered, that is circularity, roundness, aspect ratio, solidity, major axis and minor axis. However an SPSS-guided principal component analysis (PCA) revealed that the major shape descriptors were circularity, major and minor axes, explaining about 99% of the cumulative variance of dried and fresh samples data. Changes in main shape descriptors at half and end drying time for core and cortex are shown in Figure 10. In general, significant shape changes ($P \leq 0.05$) occurred during drying and these were related to the type of tissue and drying conditions. The highest were recorded in minor and major axis changes due to their radial character linking them to radial shrinkage. Consequently high positive Pearson correlation coefficients existed

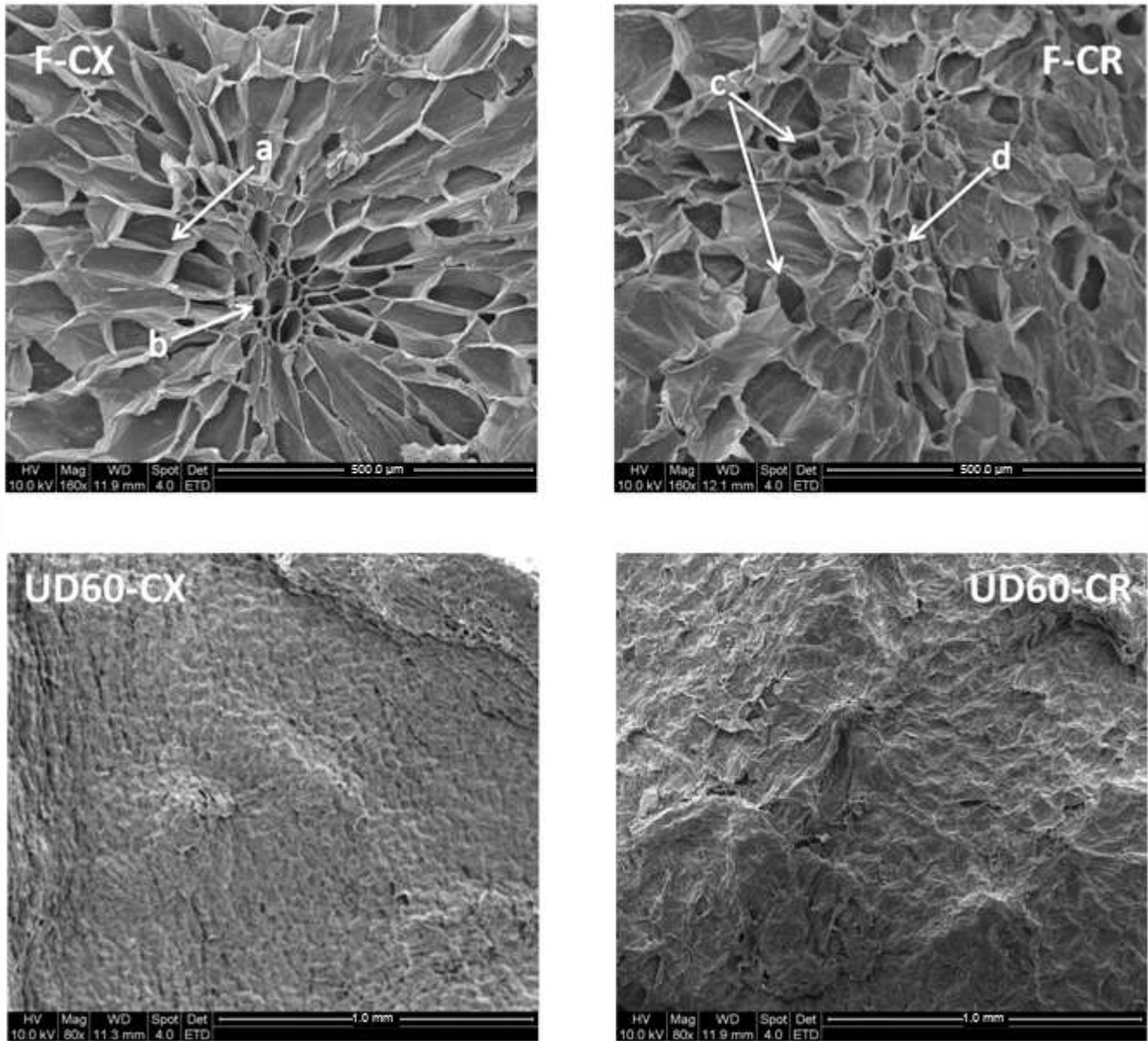


Figure 9. Microstructure of fresh (F) and dried (ud60) carrot slices. CX, cortex; CR, Core; a, parenchyma cell; b, xylem; c, Xylem tracheary elements; d, cortex-type cells around xylem trachea.

between shrinkage and major and minor axis respectively (0.940 and 0.96). At the end of drying, the Run bd60 resulted in highest shape change (67.72% for core minor axis) while ud60 recorded lower values with core circularity hitting the lowest (4.33%); ud80 shape change values ranged between those of bd60 and ud60. Figure 10 shows that blanched samples underwent higher shape changes compared to unblanched ones, which was again due to blanching-induced tissue softening as earlier discussed. Higher changes were also recorded at higher drying temperatures. All slices tested showed that the cortex circularity was always higher than that of core, explaining the existing irregularities in the pith-centered

core. The used slices were not perfectly circular since their mean value (0.92 ± 0.09) was lower to that of maximum circularity (that is 1). For all samples, Figure 10 shows that the circularity was severely lost, varying from 4.33 to 18.22% at half drying time; and from 17.79 to 50.22% at the end of drying. Hence hot air drying negatively affected the shape of carrots slices.

Color

The Hunterlab $L^*a^*b^*$ values of a product are important since they are associated with the visual color. Figure

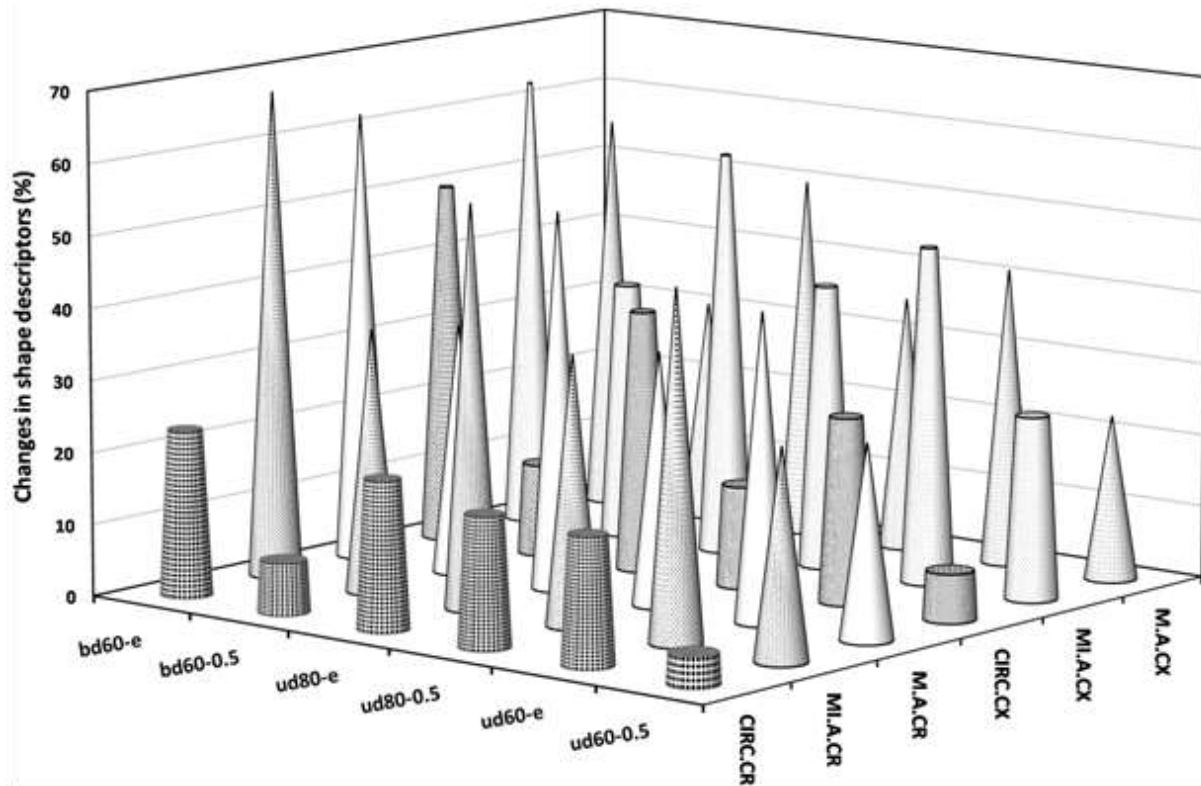


Figure 10. Changes in major shape descriptors during drying. 0.5, half drying time; e, end drying time; M.A, major axis; M.I.A, minor axis; Circ, circularity; cx, cortex; cr, core.

Table 4. Differences in visual color between fresh and dried carrot slices.

sample	Δa^*	Δb^*	ΔE^*	ΔC^*	H°
bd60	-1.02±0.92 ^d	-15.02±2.00 ^c	17.86±1.28 ^a	15.05±2.04 ^b	0.84±0.03 ^a
ud60	-6.82±0.75 ^c	-16.87±0.56 ^c	25.93±0.95 ^b	18.19±0.80 ^c	0.92±0.01 ^b
ud60cr	-1.93±0.78 ^d	-1.94±1.89 ^d	29.92±2.17 ^c	2.74±0.52 ^a	1.10±0.02 ^e
ud60cx	-16.38±0.73 ^a	-25.75±0.88 ^a	33.95±1.53 ^d	30.52±1.09 ^e	0.95±0.01 ^c
ud80	-14.71±0.32 ^b	-20.60±1.01 ^b	30.71±0.29 ^c	25.31±0.95 ^d	1.07±0.01 ^d

^{a-e}Means with different superscripts within columns are significantly different (P<0.05).

11 shows the L*a*b* color measurement results and Table 4 shows the drying-induced color differences. The color's chroma components a* and b* values for fresh whole carrot slice ranged between those of core and cortex. Furthermore, significant differences (p<0.05) between core and cortex chroma values were recorded, confirming earlier reports on non-homogenous color distribution in carrot tissues (Buishand and Gabelman, 1979). Luminosity (L*) has been used by several authors as an indicator of vegetable deterioration (Rocha et al., 2007). L* value increased during drying due to samples whitening; this was more significant in non-pretreated samples (Figure 11). Drying significantly decreased a*b* values in all samples, and increased their coefficients of variation (i.e., 33.16% for a* and 28.84% for b*). This

suggested a degradation of carrot color pigments during drying, especially carotenoids. Table 3 reveals that differences in chroma (ΔC^*) between fresh and dried samples were all pair-wisely statistically significant. The total color differences (ΔE^*) for bd60, ud60 and ud80 were also significantly different but bd60 lost lesser color than others as shown by its lowest ΔE^* (17.86±1.28). Δa^* and Δb^* values were also lower with bd60. All these results indicate that air drying deteriorated the color of carrot and that the blanching pretreatment stabilizes it as a result of consequent denaturing of oxidative enzymes during blanching. Hue angle indicates the degree of browning, and increasing yellowness results in high hue angles (Heimdal et al., 1995). As shown in Table 4, the highest hue angles were observed in ud80, followed by

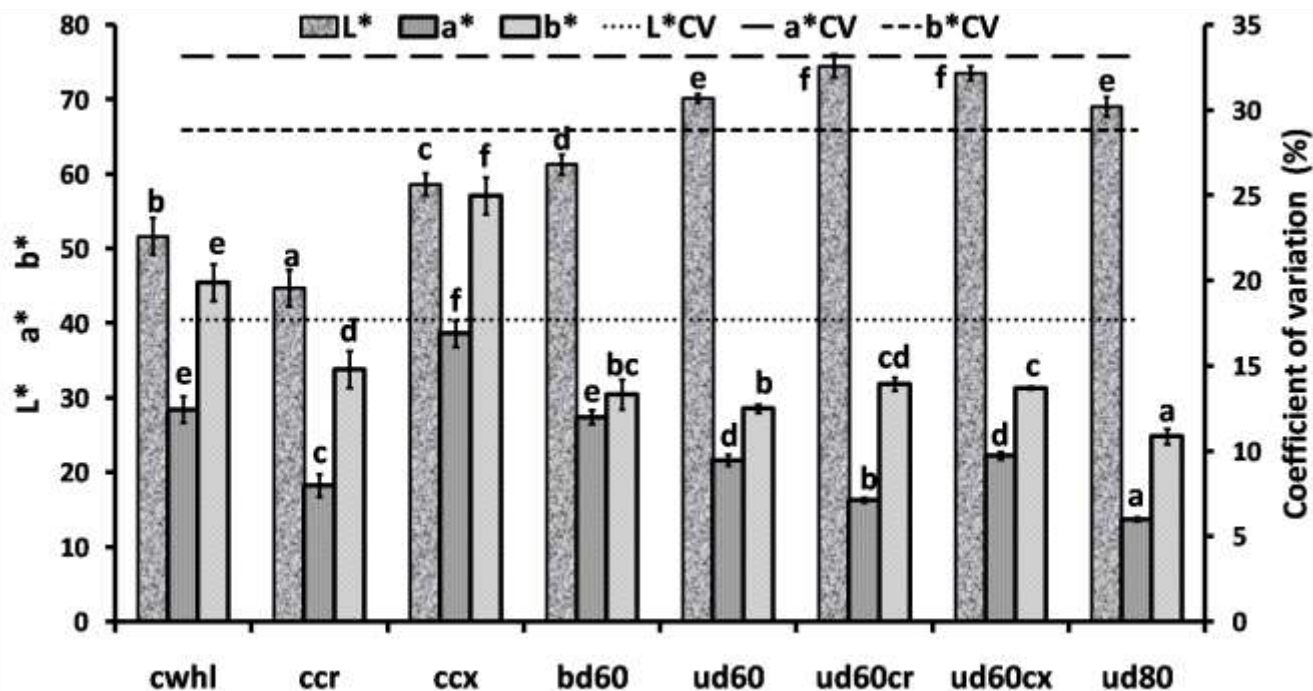


Figure 11. Hunterlab L*a*b* values and their coefficients of variation for control and dried samples. Cwahl, control-whole slice; ccr, control-core; ccx, control-cortex.

ud60 and bd60; this means that the high drying temperatures intensify browning. Furthermore scorching was seen in ud80, with accentuations in core probably due to its pronounced fibrous structure causing it to be more heat sensible than cortex.

A significant whitening process during drying was observed, with higher WI values seen in core and in unblanched-dried samples. In addition, it seemed that drying at higher temperature contributed to higher WI (Figure 12). For the fresh samples, the core whitening index was higher than that of cortex. Whitening resulted from the production of a protective layer known as 'white blush' caused by the dehydration and lignifications, where lignifications is an enzyme-stimulated reaction evaluated by the 'whiteness index' (Rocha et al., 2007). During blanching, the lignifications could not occur due to enzyme denaturation, which led to a lower WI value in blanched-dried samples. Higher drying temperatures induced higher drying rates, thus explaining the higher WI recorded during drying at 80°C.

Total carotenoid contents

Total carotenoid contents in carrots' tissues are shown in Figure 11. For fresh samples, there were significant differences in carotenoid contents between core and cortex [15.80 ± 0.02 vs. 6.60 ± 1.44 mg/100 g sample (wet basis)]; the whole slice's carotenoid contents was 11.10 ± 0.02 44 mg/100 g sample. The color differences

between the two tissues are caused by different accumulation intensities of carotene during the root's growth, where carotene is laid down first in the oldest cells of the cortex and then in the oldest cells of the core (USDA, 1940). These results also agreed with the Hunterlab L*a*b* results earlier discussed, where superior visual color quality was found in cortex. In addition, USD Release 23 showed that carotenoid contents in fresh carrots are approximately 12 mg/100 g sample; in agreement with our results. Drying caused significant decreases in carotenoid contents, where unblanched samples underwent higher carotenoids loss compared to blanched samples dried at the same temperature. Furthermore, drying unblanched samples at 80°C caused greater losses than drying them at 60°C. For example from Figure 13, it is deduced that the changes in carotenoid contents for the treatments ud60, bd60, ud80 and bd80, were respectively 35.23 ± 3.97 , 31.08 ± 9.15 , 46.42 ± 0.20 and $22.32 \pm 5.29\%$. In all samples, the dried cortex resulted in higher carotenoids contents than the dried core. In addition, the carotenoids losses in the two tissues highly varied during drying, lying between 35.55 ± 0.38 (for bd60-cortex) to $65.60 \pm 0.20\%$ (for bd60-core).

Most carrots' carotenoids are polyunsaturated and highly reactive. In the presence of catalysts, the conjugate double bonds can react with oxygen and other radicals to form carotenoid oxidation products and/or other derived products. Hot air drying environment can facilitate these types of reactions since it contains oxygen, light and heat energy; hence the lower

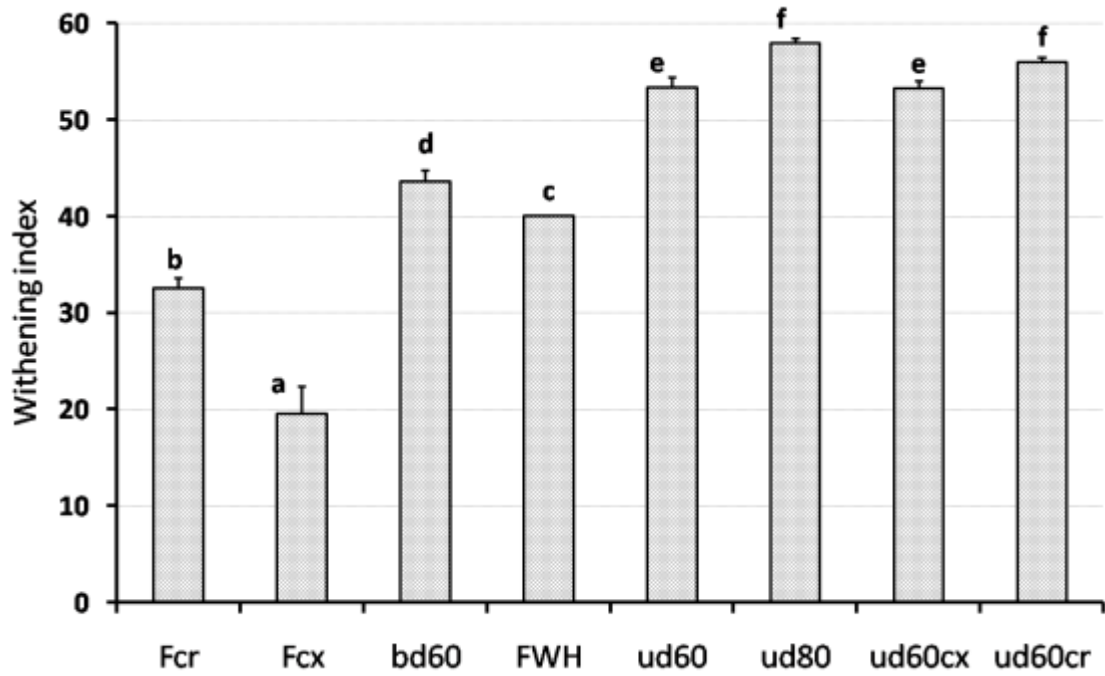


Figure 12. Whiting of carrot tissues during air drying. Fcr, fresh core; Fcx, fresh cortex; FWH, fresh whole slice.

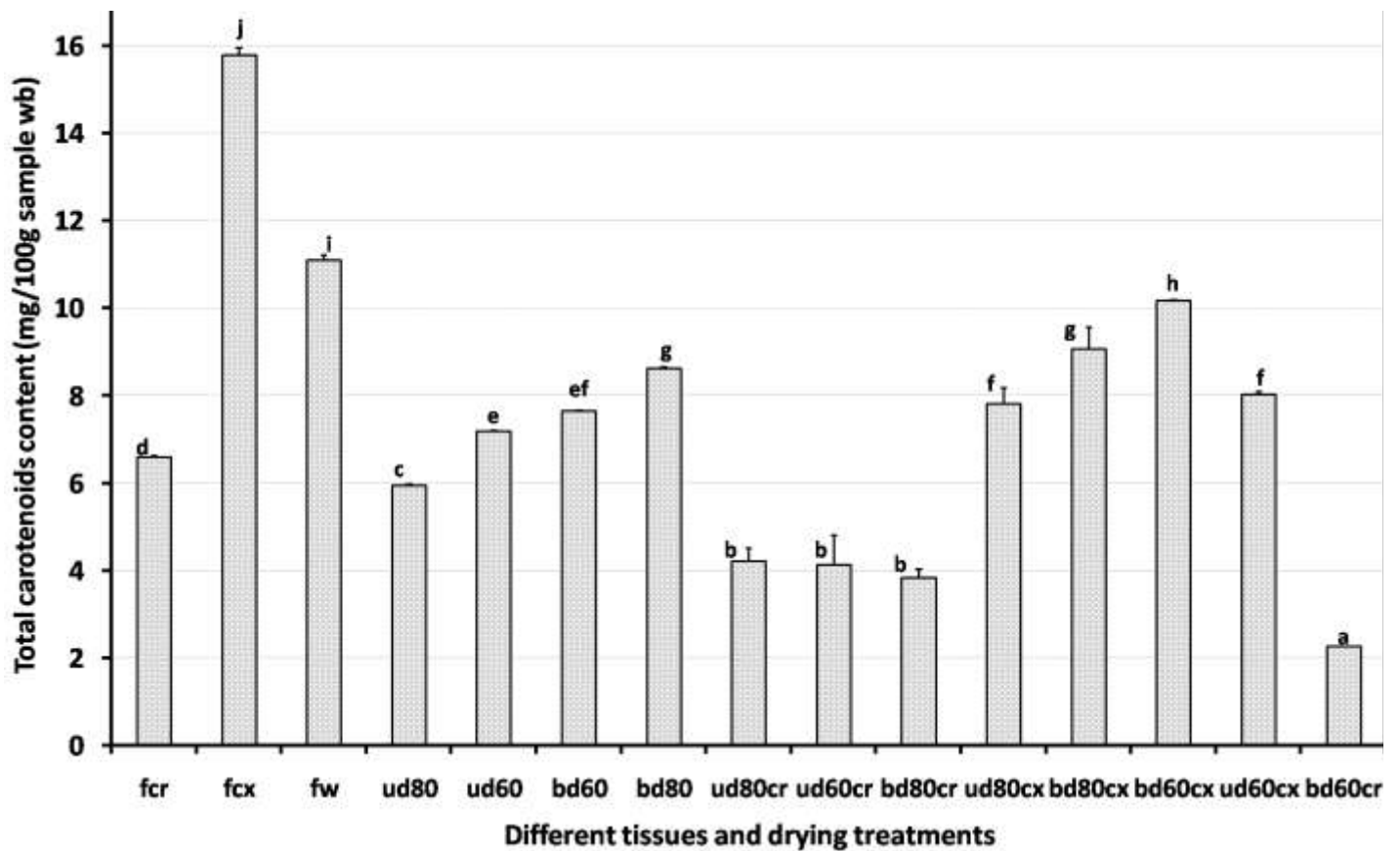


Figure 13. Effect of drying of carrots on carotenoid contents. Fcr, fcx and fw, represent respectively, the core, the cortex and the whole slice of the fresh material.

carotenoids contents observed in dried products record.

Conclusion

Effects of air drying on drying curves, radial shrinkage, and changes in visual color, shape and carotenoid contents of carrots was studied. The drying time was shortened by an hour when temperature increased from 60 to 80°C, but sample scorching was observed at 80°C. The blanching pretreatment accelerated the drying process as a result of tissue softening. For same reason, blanching-pretreatment caused samples to shrink largely compared to unpretreated samples. Shrinkage and collapse of sample structure during drying were confirmed by scanning electron microscopy. Among the mathematical models tried, only two fitted the drying data, while five fitted the radial shrinkage. A new model, the Nahimana et al. model, was tried and found to fit in category of radial shrinkage models reported in literatures. The two main carrot tissues exhibited different qualities in color, shape and carotenoid contents. The cortex of fresh and dried samples had better color due to its high chroma and low whitening index compared to the core tissue. Higher carotenoid amounts were also recorded in cortex since color is carotenoid-dependable. Significant changes in color, carotenoids and main shape descriptors of carrot slices occurred during carrots drying.

Since these qualities have been found disproportionately distributed in core and cortex, the results of this work suggest that drying separately the two heterogeneous tissues, may improve the quality of their respective dried products. Tissue separation leads to proper settings of drying conditions fitting their particular heat and mass transfer requirements, which enables proper process control for optimized quality. However this new technology would demand additional work such as; (1) new marketing studies adapting the different qualities of dried products resulting from the two carrot tissues, (2) innovation of chemical or mechanical tissue separation methods; manual separation is straightforward but laborious, which limits its application on industrial scale. Therefore, extensive tissue-driven works are still needed in carrots research.

ACKNOWLEDGEMENT

The authors gratefully acknowledge the financial support provided by the China Scholarship Council.

REFERENCES

- Aghabashlo M, Kianmehr MH, Khani S (2008). Mathematical modeling of carrot thinlayer drying using new model. *Energ. Convers Manage*, 49: 201-212.
- Banga O (1957). The development of the original European carrot material. *Euphytica*, 6: 64-76.
- Baranska M, Baranski R, Schulz H, Nothnagel T (2006). Tissue-specific accumulation of carotenoids in carrot roots. *Planta*, 22: 1028-1037.
- Buishand JG, Gabelman WH (1979). Investigations on the inheritance of color and carotenoid content in phloem and xylem of carrot roots (*Daucus carota* L.). *Euphytica*, 28: 611-632.
- Erle U (2005). Drying using microwave processing, in *The Microwave Processing of Foods*, ed. by Shubert H, and Reiger M, Cambridge: Woodhead Publishing Ltd.
- FAO/WHO (1998). Vitamin and mineral requirements in human nutrition, 2nd ed. Report of a joint FAO/WHO expert consultation, Bangkok, Thailand, 21-30 September 1998. p. 179.
- Garcia-Closas R, Berenguer A, Jose Tormo M, Jose Sanchez M, Quiros JR, Navarro C, Arnaud R, Dorronsoro M, Dolores Chirlaque M, Barricarte A, Ardanaz E, Amiano P, Martinez C, Agudo A, Gonzalez CA (2004). Dietary sources of vitamin C, vitamin E and specific carotenoids in Spain. *Br. J. Nutr.* 91: 1005-1011.
- García-Pérez JV, Cárcel JA, Riera E, Mulet A (2009). Influence of the Applied Acoustic Energy on the Drying of Carrots and Lemon Peel. *Drying Technol.* 27(2): 281-287.
- Górnicki K, Kaleta A (2007). Drying curve modeling of blanched carrot cubes under natural convection condition. *J. Food Eng.* 82: 160-170.
- Heimdal H, Kühn BF, Poll L, Larsen LM (1995). Biochemical Changes and Sensory Quality of Shredded and MA-Packaged Iceberg Lettuce. *J. Food Sci.* 60(6): 1265-1268.
- Igathinathane C, Pordesimo LO, Batchelor WD (2009). Major orthogonal dimensions measurement of food grains by machine vision using Image. *J. Food Res. Int.* 42: 76-84.
- Igathinathane C, Pordesimo LO, Columbus EP, Batchelor WD, Methuku SR (2008). Shape identification and particles size distribution from basic shape parameters using Image. *J. Comput. Electron. Agr.* 63: 168-182.
- Krokida MK, Karathanos VT, Maroulis ZB (1998). Effect of freeze-drying conditions on shrinkage and porosity of dehydrated agricultural products. *J. Food Eng.* 35: 369-380.
- Lin TM, Durance TD, Scaman CH (1998). Characterization of vacuum microwave, air and freeze dried carrot slices. *Food Res. Int.* 31: 111-117.
- Lozano JE, Rotstein E, Urbicain MJ (1983). Shrinkage, porosity and bulk density of foodstuffs at changing moisture contents. *J. Food Sci.* 48: 1497-502.
- Maté JI, Zwietering M, Riet VK (1999). The effect of blanching on the mechanical and rehydration properties of dried potato slices. *Eur. Food Res. Technol.* 209: 343-347.
- McLaren K (1980). CIELAB Hue-Angle Anomalies at Low Tristimulus Ratios. *Color Res. Appl.* 5: 139-143.
- Metzger BT, Barnes DM, Reed JD (2008). Purple carrot (*Daucus carota* L.) polyacetylenes decrease lipopolysaccharide-induced expression of inflammatory proteins in macrophage and endothelial cells. *J. Agric. Food Chem.* 56: 3554-3560.
- Nahimana H, Zhang M (2011). Shrinkage and color change during microwave vacuum drying of carrot. *Drying Technol.* 29(7): 836-847.
- Nahimana H, Zhang M, Mujumdar AS, Ding Z (2011). Mass transfer modeling and shrinkage consideration during osmotic dehydration of fruits and vegetables. *Food Rev. Int.* 27: 1-26.
- Ozdemir M, Devres YO (1999). The thin layer drying characteristics of hazelnuts during roasting. *J. Food Eng.* 42: 225-233.
- Pisani P, Berrino F, Macaluso M, Pastorino U, Crosignani P, Baldasseroni A (1986). Carrots, green vegetables and lung cancer: a case-control study. *Int. J. Epidemiol.* 15: 463-468.
- Prabhanjan DG, Ramaswamy HS, Raghavan GSV (1995). Microwave-assisted convective air drying of thin layer carrots. *J. Food Eng.* 25: 283-293.
- Rangana S (1977). *Manual of Analysis of Fruit and Vegetable Products*. pp. 84-88.
- Rasband WS (2010). ImageJ, US National Institutes of Health, Bethesda, Maryland, USA, <http://rsb.info.nih.gov/ij/index.html> [accessed 5July, 2010].
- Rocha AMCN, Ferreira JFFC, Silva ÂMM, Almeida GN, Morais AMMB (2007). Quality of grated carrot (*var. Nantes*) packed under vacuum. *J. Sci. Food Agric.* 87: 447-451.
- Rodieck B (2008). Ellipse Fitter class of ImageJ. <http://rsb.info.nih.gov/ij/developer/source/ij/process/EllipseFitter.java.html>.

- Romano G, Kocsis L, Farkas I (2009). Analysis of energy and environmental parameters during solar cabinet drying of apple and carrot. *Drying Technol.* 27(4): 574-579.
- Schulz DG, Köpke U (1992). Determining the quality of organic produce, extended quality parameters and quality index, in *Proceedings 9th IFOAM Conference*, pp. 338-348.
- Singh B, Panesar PS, Gupta AK, Kennedy JF (2007). Optimisation of osmotic dehydration of carrot cubes in sucrose-salt solutions using response surface methodology. *Eur. Food Res. Technol.* 225: 157-165.
- Smith BG, James BJ, Ho CAL (2007). Microstructural characteristics of dried carrot pieces and real time observations during their exposure to moisture. *Int. J. Food Eng.* 3(4): 7.
- Suzuki K, Kubota K, Hasegawa T, Hosaka H (1976). Shrinkage in dehydration of root vegetables. *J. Food Sci.* 41: 1189-1193.
- Thompson R (1969). Some factors affecting carrot root shape and size. *Euphytica* 18: 277-285.
- USDA (1940). Description of types of principal American varieties of orange-fleshed carrots. *Miscellaneous publications*, p. 361.
- Van Meel DA (1958). Adiabatic convection batch drying with recirculation of air. *Chem. Eng. Sci.* 9: 36-44.
- Watzl B, Bub A, Briviba K, Rechkemmer G (2003). Supplementation of a low-carotenoid diet with tomato or carrot juice modulates immune functions in healthy men. *Ann. Nutr. Metab.* 47: 255-261.
- Witrowa-Rajchert D, Bawoł A, Czapski J, Kidoń M (2009). Studies on drying of purple carrot roots. *Drying Technol.* 27(12): 1325-1331.